Cancer Letters 451 (2019) 110–121

Contents lists available at ScienceDirect

Cancer Letters

journal homepage: www.elsevier.com/locate/canlet

Original Articles

Phosphorylation of LIFR promotes prostate cancer progression by activating the AKT pathway

Jialiang Shao[a,b,1], Wencheng Zhu[c,1], Yufeng Ding[d,1], Hongwen Zhu[e,****], Xiaoqian Jing[f], Hua Yu[a], Mujun Lu[d], Yunbo Qiao[a,***], Xiang Wang[b,**], Hua Ai[g,h], Xiongjun Wang[a,*]

[a] Precise Genome Engineering Center, School of Life Sciences, Guangzhou University, Guangzhou, 510006, China
[b] Department of Urology, Shanghai General Hospital, Shanghai Jiaotong University, Shanghai, 200080, China
[c] Shanghai Institute of Biochemistry and Cell Biology, Chinese Academy of Sciences, 320 Yue Yang Road, Shanghai, 200031, China
[d] Department of Urology and Andrology, Ren Ji Hospital, School of Medicine, Shanghai Jiao Tong University, Shanghai, 200001, China
[e] Shanghai Institute of Materia Medica, Chinese Academy of Sciences, Shanghai, 201203, China
[f] Department of Surgery, Ruijin Hospital, Shanghai Jiao Tong University School of Medicine, Shanghai, 200025, China
[g] National Engineering Research Center for Biomaterials, Sichuan University, Chengdu, 610065, China
[h] Department of Radiology, West China Hospital, Sichuan University, Chengdu, 610065, China

ARTICLE INFO

Keywords:
LIFR
Phosphorylation
Prostate cancer
AKT

ABSTRACT

Prostate cancer (PCa) is the most common solid organ malignancy among men, outnumbering both lung and colorectal cancer, and it is the second leading cause of male tumor-related death in the United States due to high metastasis. Recently, leukemia inhibitory factor receptor (LIFR) has been found to play roles in multiple types of cancer. However, the roles of LIFR in the progression of PCa remain to be revealed. In this study, we found that LIFR plays an oncogenic role in PCa. The phosphorylation of LIFR at S1044 contributes to subsequent activation of the AKT pathway, inducing the expression of a series of proliferation and metastatic genes. Additionally, LIFR-S1044 is phosphorylated by ERK2 but not ERK1. The signal intensity of pLIFR-S1044 and pAKT S473 in PCa tissue displays a tight positive correlation. The ERK2/LIFR/AKT axis modulates PCa progression and offers a promising therapeutic and diagnostic target for PCa.

1. Introduction

Prostate cancer (PCa) is the most common solid organ malignancy and the second leading cause of cancer-related death in men in the United States [1]. Frequently, metastasis makes predominant contributions to the high recurrence and mortality rates of PCa [2]. However, the molecular mechanisms underlying PCa metastasis and progression remain largely unknown [3]. Therefore, there is a tremendous need for the development of mechanism-based strategies by which PCa could be treated with better outcomes.

Leukemia inhibitory factor receptor (LIFR) is an integral component of the glycoprotein 130 (gp130)-LIFR complex and participates in signal transduction through the IL-6 cytokine family [4,5]. There are two forms of LIFR, the membrane-bound form, LIFR, and the soluble form, sLIFR, which have antagonistic effects on each other [6]. When LIFR binds to its ligand (LIF), the LIF/LIFR complex heterodimerizes with gp130 and thereby activates several signaling pathways in different cell types, including the Janus protein tyrosine kinase (JAK)-signal transducer and activator of transcription (STAT)3, mitogen-activated protein kinase (MAPK), and phosphoinositol 3-kinase (PI3K) pathways [7,8].

LIFR has been found to act as a tumor suppressor in multiple types of cancer, such as breast, liver, gastric and colorectal cancers. In breast cancer, LIFR promotes the localization of Scribble to the cell membrane,

Abbreviations: PCa, prostate cancer; LIFR, leukemia inhibitory factor receptor; JAK, Janus protein tyrosine kinase; STAT, signal transducer and activator of transcription; MAPK, mitogen-activated protein kinase; PI3K, phosphoinositol 3-kinase; CCK-8, Cell Counting Kit-8; LC-MS/MS, liquid chromatography coupled with tandem mass spectrometry; shRNA, short hairpin RNA; BLI, bioluminescence imaging

* Corresponding author.
** Corresponding author.
*** Corresponding author.
**** Corresponding author.
E-mail addresses: zhw@simm.ac.cn (H. Zhu), ybqiao@gzhu.edu.cn (Y. Qiao), drseanwang@163.com (X. Wang), xjwang02@sibcb.ac.cn (X. Wang).
[1] These authors contributed equally to this work.

https://doi.org/10.1016/j.canlet.2019.02.042
Received 15 December 2018; Received in revised form 31 January 2019; Accepted 18 February 2019

which in turn activates hippo signaling, leading to the phosphorylation and functional inactivation of the transcriptional coactivator Yes-associated protein 1 (YAP1), thus suppressing tumor metastasis [9,10]. Activation of LIFR is also involved in inducing breast cancer cell into a dormancy phenotype which reduces bone metastasis [11]. In addition, LIFR downregulation is significantly correlated with poor clinical outcomes in breast cancer patients [10]. In hepatic and gastric cancers, LIFR was detected as a novel suppressor gene that acts by negatively regulating the PI3K/AKT pathway [12–14]. Moreover, *LIFR* has been shown to be epigenetically silenced through DNA methylation in liver cancer cells [15]. Recently, there is some new evidence that LIFR may act as an oncogene. In colorectal cancer, LIFR promotes tumor angiogenesis by upregulating IL-8 [16]. LIFR displayed a pro-metastatic role in melanoma [17]. In PCa, *LIFR* is epigenetically upregulated by histone methyltransferase KMT2D to sustain carcinogenesis and metastasis [18]. However, the oncogenic mechanism of LIFR in PCa remains to be determined.

In the present study, we verified that LIFR could promote prostate cancer cell growth and metastasis *in vitro* and *in vivo*. Interestingly, we found that LIFR protein level displays no significant difference between PCa and adjacent tissues. However, LIFR phosphorylation at S1044 was obviously upregulated in PCa tissue and was positively related to PCa progression and metastasis. Furthermore, the activation of LIFR, which was phosphorylated by ERK2 at S1044, is required to promote prostate cancer progression and PI3K-AKT pathway regulation. Thus, our results determined that LIFR plays an oncogenic role in prostate cancer by regulating PI3K-AKT pathway. The phosphorylation of LIFR at S1044, considered LIFR activation, could be a promising therapeutic target and prognostic marker in PCa.

2. Materials and methods

2.1. Patients

This study was approved by the institutional review board of Shanghai General Hospital, Shanghai Jiaotong University. Each patient signed the informed consent form. From January 2005 to December 2015, 261 consecutive patients were newly diagnosed with localized or metastatic PCa at the Department of Urology. All patients referred to our institution with a new diagnosis of PCa (Gleason score ≤ 9) underwent laparoscopic radical prostatectomy (LRP). Pathological results were adenocarcinoma of the prostate. All specimens were collected half an hour postoperatively.

2.2. Immunohistochemistry (IHC) staining

The diagnoses of these prostate cancer samples were verified by pathologists. The use of these tissue materials for research was approved by the Shanghai General Hospital. We rated the intensity of staining on a scale of 0–3: 0, negative; 1, weak; 2, moderate; and 3, strong. We assigned the following proportion scores: X means X% of the tumor cells were stained ($0 \leq X \leq 100$). The score (H-score) was obtained by the formula: $3 \times$ percentage of strongly staining nuclei $+ 2 \times$ percentage of moderately staining nuclei $+ 1 \times$ percentage of weakly staining nuclei, giving a range of 0–300. Scores were compared with overall survival, defined as the time from the date of diagnosis to death or last known date of follow-up. The detailed information of Post-Operative Outcomes Between pS1044-high and pS1044-low tumors was listed in Table 1.

2.3. Cell culture, antibodies, plasmids and cell transfection

PC-3, VCaP and HEK293T cells were used in this study. PC-3 and VCaP cells were cultured in RPMI 1640 medium supplemented with 10% fetal calf serum (Gibco), while HEK293T cells were cultured in DMEM supplemented with 10% fetal calf serum (Gibco).

Table 1
Post-operative outcomes between pS1044-high and pS1044-low tumors.

Biochemical Recurrence, n (%)	pS1044-high		pS1044-low		p-Value
	N	%	N	%	
No	33	31.7	102	64.9	< 0.001 ($X^2 = 27.7$)
Yes	71	68.3	55	35.1	
ADT, n (%)				Z = −10.6	< 0.001
None/Unknown	43	41.3	102	64.9	
Salvage	28	26.9	43	27.3	
For Metastatic Disease	33	31.8	12	7.8	
XRT, n (%)				Z = −10.3	< 0.001
None/Unknown	71	68.2	124	79.0	
Salvage	29	27.9	30	19.1	
For Metastatic Disease	4	3.9	3	1.9	
Metastasis, n (%)					< 0.001
No Metastasis	39	37.5	127	80.9	
Clinical Metastasis	65	62.5	30	19.1	
Cancer-Specific Survival, n (%)				$X^2 = 48.8$	< 0.001
Alive	59	56.7	146	92.9	
Dead from PCa	45	43.3	11	7.1	
Overall Survival, n (%)				$X^2 = 41.9$	< 0.001
Alive	49	47.1	133	84.7	
Dead	55	52.9	24	15.3	

Plasmids: All of the Flag-tagged plasmids were constructed using the pCDNA3.0 vector. The lentiviral plasmids for overexpressing LIFR or its mutants were constructed using the pWPI vector.

Antibodies: antibodies against FLAG (sc-166355), LIFR (sc-659) and β-actin (sc-47778) were purchased from Santa Cruz Biotechnology, Inc.; FLAG M2 beads (F2426) were purchased from Sigma (Sigma-Aldrich Co., LLC); antibodies against AKT (#4685), pAKT-S473 (#4060), YAP (#14074), pYAP–S127 (#13008), ERK (#5013), and pERK-T202/204 (#4370) were purchased from Cell Signaling Technology.

Cell transfection was performed with Lipofectamine™ 2000 (Invitrogen) according to the manufacturer's instructions. siRNAs against ERK1 (SignalSilence® p44 MAPK siRNA) and ERK2 (SignalSilence® pool p42 MAPK siRNA) were purchased from Cell Signaling Technology.

2.4. Cell proliferation

Cell proliferation was measured using the Cell Counting Kit-8 (CCK-8, Dojindo Laboratories, Kumamoto, Japan), according to the manufacturer's instructions. The constructed stable cell lines were seeded in a 96-well plate and then cultured at 24-h intervals for 5 days. Cell viability was then measured using the CCK-8 assay. Absorbance was measured at 450 nm as an indicator of cell viability. All experiments were independently repeated at least 3 times.

2.5. Transwell and invasive assays

Transwell assay was performed using FalconTM Cell Culture Insert (BD353097) according to the manufacturer's instructions. For invasion assay, matrigel-coated chambers (BD Biosciences, USA) containing 8 μm pores were used. Briefly, 2×10^5 serum-starved cells were seeded into the upper chambers in serum-free medium. The lower chambers were filled with culture media containing 10% FBS as a chemo-attractant. After 48 h of incubation, the remaining cells in the upper chamber were removed by cotton swabs. These cells on the lower surface of the membrane were fixed in 4% paraformaldehyde and stained with 0.5% crystal violet. Cells in at least 3 random microscopic fields (magnification, $\times 10$) were counted and photographed. All experiments were performed in duplicates and repeated 3 times.

2.6. Adhesion assay

Approximately 2×10^5 cells were harvested, resuspended in complete medium and then seeded onto a 24-well plate precoated with matrix proteins (20 μg/ml fibronectin or 20 μg/ml laminin). After the cells were incubated for 1 h, they were washed twice with PBS to remove non-adherent cells. The bound cells were quantified by a WST-1 assay (Roche, Mannheim, Germany) at a wavelength of 450 nm in a microplate reader. The change in optical density was represented as a fold of the control.

2.7. Immunoprecipitation and western blot/immunoblot analysis

For the immunoprecipitation analysis, PC-3 cell lysates (10 mg of protein) were mixed with the indicated antibody (2 μg) at 4 °C for 4 h, followed by the addition of 50 μl of protein G–Sepharose (Roche) and incubation overnight at 4 °C. Immune complexes were washed five times with lysis buffer (Millipore) supplemented with complete mini-protease inhibitor cocktail (Roche). After boiling in 3× loading buffer (25 mmol/L Tris, pH 6.8, 1% SDS, 5 mmol/L EDTA), the samples were subjected to SDS-PAGE and transferred to nitrocellulose membranes using the iBlot Dry Blotting System (Bio-Rad). After blocking with PBS containing 5% nonfat milk, the nitrocellulose membranes were immunoblotted with the indicated primary antibodies, including anti-FLAG (Sigma) and pLIFR-S1044 (Willget Biotech Co., LTD).

To detect the signaling pathway, 25 μg of PC-3 cell lysate was subjected to SDS-PAGE and blotted with anti-FLAG, anti-YAP, anti-pYAP, anti-AKT, anti-pAKT, anti-ERK, anti-pERK, and anti-β-actin, followed by incubation with the appropriate horseradish-peroxidase-conjugated secondary antibodies (Santa Cruz Biotechnology). Bands were visualized by enhanced chemiluminescence (Pierce).

2.8. Immunoprecipitation and LC-MS/MS

FLAG mouse monoclonal antibody-coated beads were incubated with FLAG-LIFR cell lysate for 4 h. Purified FLAG-LIFR and its associated complexes were boiled at 95 °C for 8 min and then loaded into SDS-PAGE gels for the separation of FLAG-LIFR and its associated proteins. The FLAG-LIFR band, representing modified LIFR, was cut off from the gel and processed through a series of routine procedures, including reductive alkylation, trypsin digestion and peptide extraction. The peptides were analyzed by LC-MS/MS on a Q Exactive™ mass spectrometer (Thermo Fisher Scientific). Proteins were identified by comparing the fragment spectra against those in the National SWISS-PROT protein database (EBI) using Mascot Server 2.4 (Matrix Science). Phospho-peptide matches were analyzed using MaxQuant v1.5.2.8 implemented in Proteome Discoverer and manually curated.

2.9. Quantitative real-time PCR

Total RNA was extracted with an RNA High-Purity Total RNA Rapid Extraction Kit (Qiagen). cDNA was prepared using oligonucleotide (dT), random primers, and a Thermo Reverse Transcription Kit (Roche). Quantitative real-time PCR was performed using 2 × SYBR real-time PCR Premixture (Roche) under the following conditions on an ABI Prism 7700 sequence detection system: 5 min at 95 °C followed by 40 cycles at 95 °C for 30 s, 55 °C for 40 s, and 72 °C for 1 min. Data were normalized to the expression of a control gene (β-actin) for each experiment. The primer pairs used for quantitative real-time PCR are listed in Supplementary Table 1.

2.10. RNA-seq and analysis

Total RNA was extracted for RNA sequencing using an Illumina sequencer with a HiSeq 2500 instrument. Sequencing data analysis and management were performed with BaseSpace Sequence Hub. Kyoto Encyclopedia of Genes and Genomes (KEGG) pathway analysis revealed the top 10 pathways. A full list of KEGG pathway analysis is in Supplementary Table 2.

2.11. In vivo tumor xenograft and metastatic model

Five-to seven-week-old BALB/c nude mice were purchased from the Shanghai Institute of Material Medica, Chinese Academy of Sciences (Shanghai, China). For xenograft implantation, indicated PC-3 cells (1×10^6) were subcutaneously injected into the left dorsal part of mice. The tumors were measured every three days with microcalipers and tumor volume was measured using tumor length (L) and width (W) and calculating the volume with the formula $LW^2/2$. Tumors were dissected for further analyses. For metastatic model, the mice received an intracardiac injection of 10^6 PC-3 cells. Bioluminescence imaging (BLI) was performed with a NightOWL II LB 983 Imaging System (Berthold). Bone damage was detected by X-ray radiography using a Faxitron instrument (Faxitron Bioptics) and quantified using ImageJ software.

2.12. Statistical analysis

All results were presented as the mean ± standard error of mean (SEM), unless stated otherwise. Statistical analysis was performed using GraphPad Prism Version 7.04 (GraphPad Software, Inc.). Unpaired Student's t-tests were used to determine the statistical significance of differences between the experimental groups. A p-value of < 0.05 was considered significant. Two-way ANOVA was used to analyze cell growth data. Pearson's correlation analyses were used to calculate the regression and correlation between two groups. Log-rank test was used to measure the patient survival.

3. Results

3.1. LIFR is required for the proliferation and metastasis of PCa cells in vitro and in vivo

PC-3 and VCaP are classical androgen independent and dependent PCa cell lines, respectively. To identify the role of LIFR in PCa, we generated PC-3 and VCaP cell lines with stably knocked down LIFR expression by introducing nontargeting shRNA (shNT) or LIFR shRNA (shLIFR). The LIFR knockdown efficiency was tested by western blot (Fig. 1A, left panel). The depletion of LIFR reduced the PCa cell proliferation, as measured by CCK-8 assay (Fig. 1A, right panel). More importantly, the loss of LIFR had a dramatic effect on the metastatic ability of PCa cells *in vitro*, as measured by transwell, invasion and adhesion assays (Fig. 1B). Furthermore, a xenograft study, performed by injecting PC-3 shNT or shLIFR cells into the left dorsal of nude mice, proved that LIFR also contributed to tumor growth *in vivo* (Fig. 1C). Ki67 staining confirmed that the depletion of LIFR reduced the cell proliferation rate *in vivo*, which was consistent with the CCK-8 data in Fig. 1A (Fig. 1D). Next, we conducted an intracardiac injection assay to determine whether LIFR regulated tumor metastasis to the bone *in vivo*. PC-3 cells stably expressing the luciferase gene were used to visualize metastatic lesions via bioluminescent imaging (BLI). At 2 months after inoculation, BLI data showed that tumor cells expressing shNT had metastasized to the skeleton, whereas significantly fewer LIFR-depleted cells were found in the bone (Fig. 1E). The decreased osteolysis in the LIFR-depleted group supported the results (Fig. 1F). Hematoxylin-eosin (H&E) staining confirmed the less colonized tumor foci within the skeleton in the LIFR-depleted group (Fig. 1G), indicating that LIFR depletion impaired PCa cell metastasis to the bone. Taken together, these results demonstrate that LIFR is required for PCa cell proliferation and metastasis *in vitro* and *in vivo* and this contribution might be independent of androgen signaling as PC-3 and VCaP are androgen independent and dependent PCa cells, respectively.

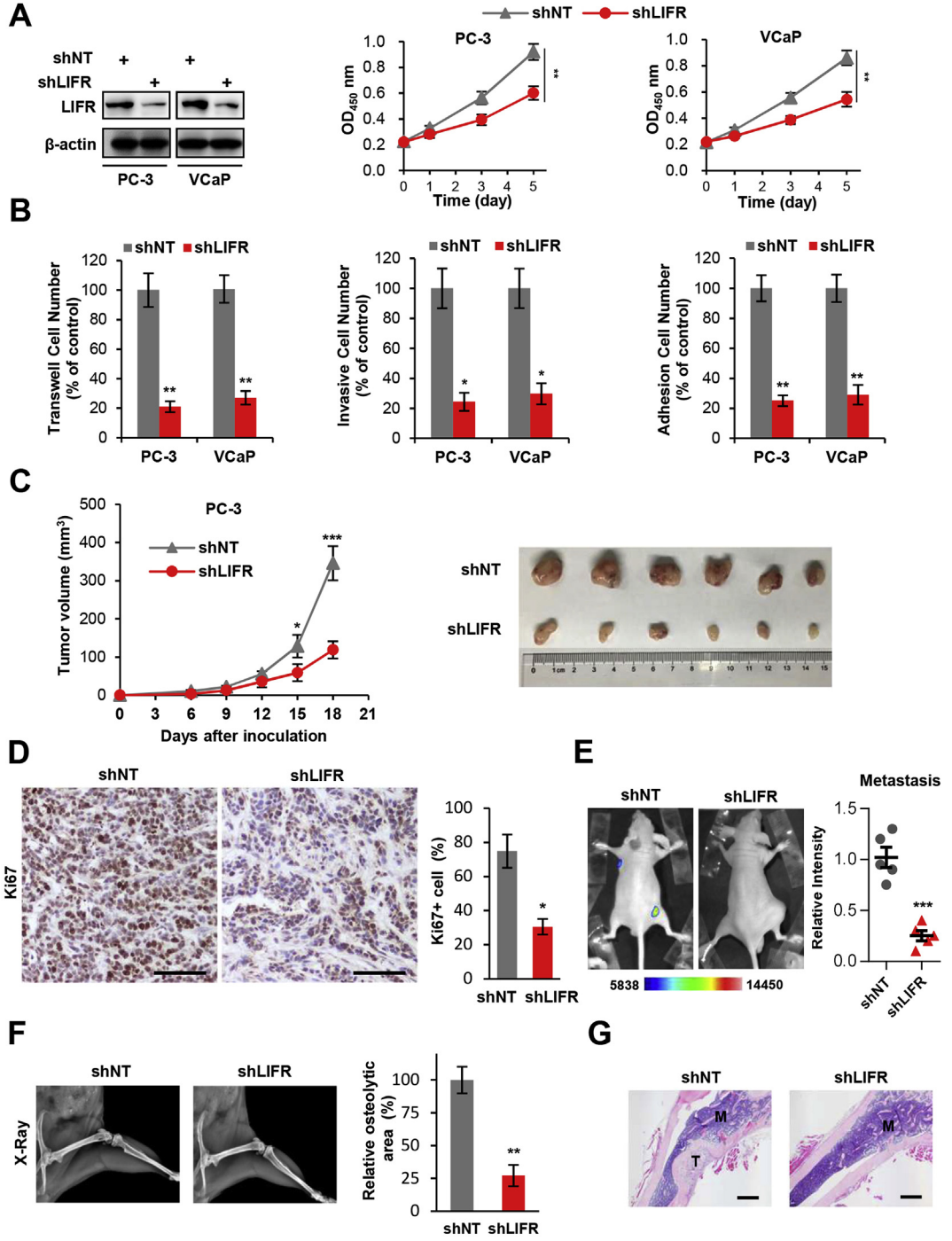

Fig. 1. LIFR is required for PCa cell proliferation and metastasis *in vitro* and *in vivo*. (A) Western blot of cell lysates (left) and measurement of cell growth (right) in control (shNT) and LIFR knockdown PC-3 or VCaP cells. **(B)** The metastatic capacity of shNT and shLIFR cells was measured by transwell, invasion and adhesion assays. **(C)** PC-3 cells stably expressing shNT or shLIFR were injected into the left dorsal part of randomized nude mice (n = 6). After injection of the tumor cells, tumor growth was examined every 3 days starting on the 6th day (left). At end of the experiment, the tumors were dissected and presented (right). **(D)** Ki67 staining of the xenograft samples was analyzed (left). Positive Ki67 staining in randomly selected sections was calculated and analyzed with corresponding p-values (right). Scale bar: 100 μm. **(E)** Representative BLI images from the shNT and shLIFR groups. Relative BLI quantitation of limb metastasis is shown in the right panel (n = 5 per group). **(F)** Representative X-ray images for assessing bone metastasis are shown in the left panel, and quantified osteolytic areas are shown in the right panel (n = 5 per group). **(G)** Images of H&E-stained bone sections from the mice, as indicated. T, tumor; M, bone marrow. Scale bar: 200 μm. Data are from three independent experiments, presented as the mean ± SEM and were analyzed by unpaired t-tests or two-way ANOVA. *p < 0.05; **p < 0.01; ***p < 0.001.

3.2. LIFR expression is not significantly associated with PCa progression

To clarify whether LIFR expression is associated with the clinical behaviors of PCa, we searched for information relating LIFR expression and clinical prognosis in a public database (UALCAN) [19]. Unexpectedly, transcription analyses of The Cancer Genome Atlas (TCGA) prostate carcinoma RNA-sequencing data showed that LIFR mRNA levels in tumor tissues were lightly less than that in normal prostate tissues (Fig. 2A). Further, there is no significant difference in the LIFR mRNA levels between tumor tissues and paired adjacent

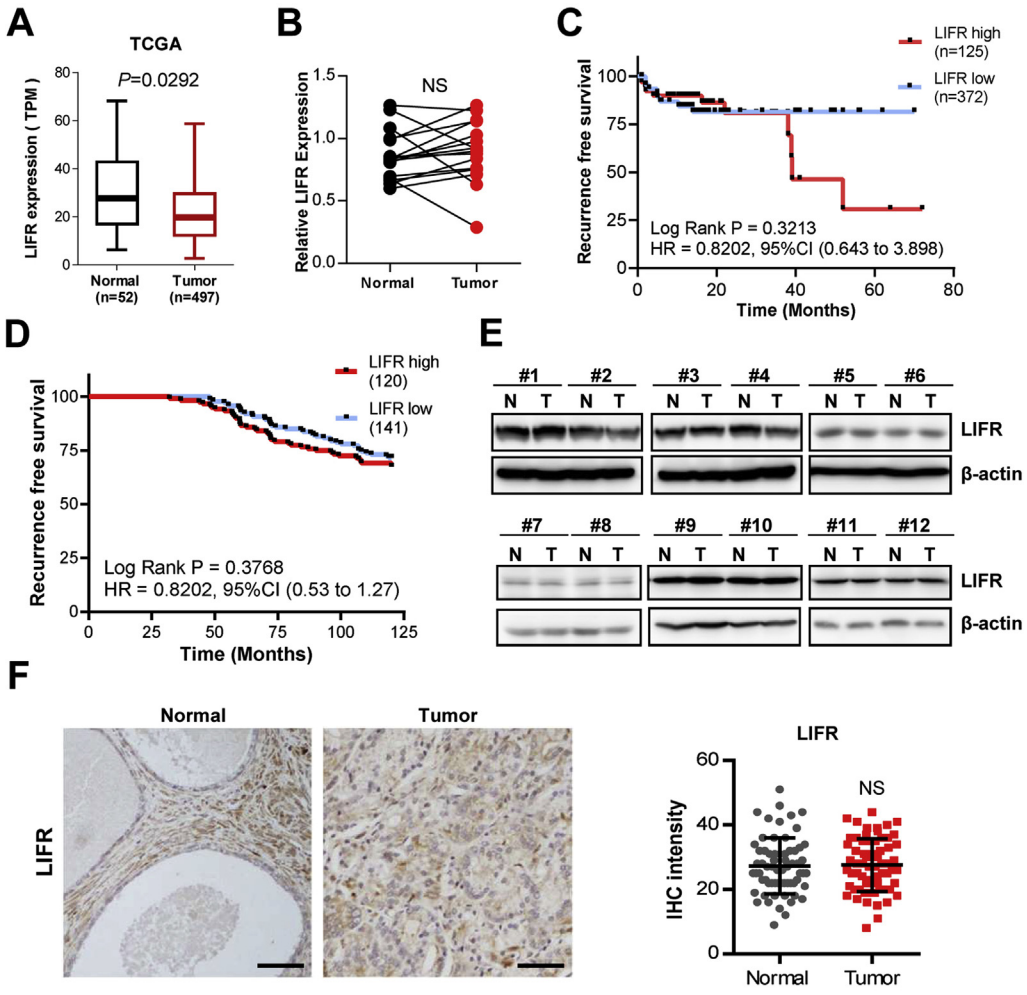

Fig. 2. LIFR expression is not significantly associated with PCa progression. (A) TCGA RNA-seq data of prostate adenocarcinoma patients were analyzed using UALCAN (http://ualcan.path.uab.edu). LIFR transcription compared in cohorts of normal prostate counterparts and primary prostate tumors was shown. **(B)** Relative LIFR expression compared between patients with primary or metastatic tumors was shown (n = 16). **(C)** The survival durations of 497 prostate adenocarcinoma patients (from TCGA) with low (n = 372, blue curve) and high LIFR expression (n = 125, red curve) were compared (p values by log-rank test). **(D)** The survival durations of 261 prostate adenocarcinoma patients in our cohort with low (n = 141, blue curve) and high LIFR expression (n = 120, red curve) were compared. **(E)** Total LIFR protein in prostate adenocarcinoma and paired adjacent normal tissues from 12 patients were tested by western blotting. β-actin was used as an internal control. **(F)** LIFR staining index in prostate adenocarcinoma and paired adjacent normal tissues from 65 patients (Wilcoxon signed-rank test). Scale bar: 100 μm *p < 0.05; **p < 0.01; ***p < 0.001; NS, not significant. (For interpretation of the references to color in this figure legend, the reader is referred to the Web version of this article.)

normal tissues collected in our hospital as well (Fig. 2B). As expected, TCGA data showed that no correlation between PCa patient survival and LIFR mRNA level, with a p value = 0.3213, indicating LIFR mRNA expression has no significance in the prognosis of PCa (Fig. 2C), which is also confirmed by PCa patient data from our hospital (Fig. 2D). The LIFR protein level in tumor tissues was also similar to that in paired adjacent normal tissues (Fig. 2E). Next, we detected LIFR distribution in PCa tissues and paired adjacent normal tissues. As shown in Fig. 2F, the representative IHC images displayed equal intensities of LIFR in PCa tissues and paired adjacent normal tissues and LIFR distributed in the membrane and cytosol. Thus, these results indicate that LIFR expression has not significant clinical relevance and it cannot be applied in the clinical diagnosis of PCa. There are other four receptor complexes for the IL-6 cytokine family signal transduction, which are IL-6R, IL-11R, CNTFR and OSMR [5]. We further searched their expression levels in normal prostate tissues and PCa (UALCAN) [19] and found that despite three out of four receptors showed significant down-regulation in PCa but none of them correlates to patient survival (Fig. S1). It is known that the post-translation modifications (PTMs) of such receptors play essential roles in their signal transduction [20]. Therefore, we speculate that the activity of LIFR, rather than the expression level of LIFR, promotes the proliferation and metastasis of PCa.

3.3. Identification of LIFR phosphorylation at S1044 in PC-3 and VCaP cells

LIFR is a type I cytokine receptor that transduces signals through a ternary receptor complex consisting of the cognate receptor and either the IL-6 signal transducer gp130 or the oncostatin M-specific receptor β subunit, which then activates the JAK/STAT, Ras/Raf/MAPK and PI3K/PKB signaling pathways [21]. In general, the intracellular segment of the IL-6 receptor will produce multiple translational modifications, including phosphorylation and acetylation, which play critical roles in further signal transduction and cancer development. The PTM is important for protein activity regulation [22], whether there is the possibility that the PTM of LIFR is the key factor of its activity and oncogenic functions. In order to test the conjecture, we transfected FLAG-LIFR plasmid into PC-3 cells to determine whether serine phosphorylation occurs in the LIFR C-terminal domain (Fig. S2). Trypsin digestion was performed in the gel to process the FLAG-LIFR proteins into peptides, which were then analyzed by tandem mass spectrometry. Three independent batches of FLAG-LIFR proteins were processed by tandem mass spectrometry to identify serine phosphorylation sites and their presence in the LIFR C-terminal domain. Among the five serine sites, S927, S1041, S1044, S1059 and S1077, S1044 phosphorylation appeared three times (Fig. 3A). We have previously generated an antibody specifically against LIFR phosphorylated at S1044 [23]. Again, we confirmed the specificity of the antibody against pS1044 by transfecting FLAG-LIFR (including wild-type and S1044A mutant plasmids) into PC-3 and VCaP cells (Fig. 3B). The spectrum of pLIFR-S1044 peptide was extracted and is presented in Fig. 3C. Furthermore, we generated stably rescued wild-type LIFR cells and S1044A mutant LIFR shLIFR cells. The expression of rescued wild-type LIFR or S1044A mutant LIFR was normalized to the endogenous LIFR expression level in shNT cells (Fig. 3D). It has been previously reported that pLIFR-S1044 is the major phosphorylation site in human LIFR upon LIF simulation

A

Identification of serine phosphorylation in LIFR C terminal

Position	S927	S1041	S1044	S1059	S1077
Numbers	3	3	3	3	3
Occurrences	1	1	3	0	2

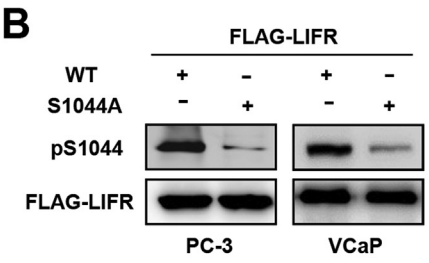

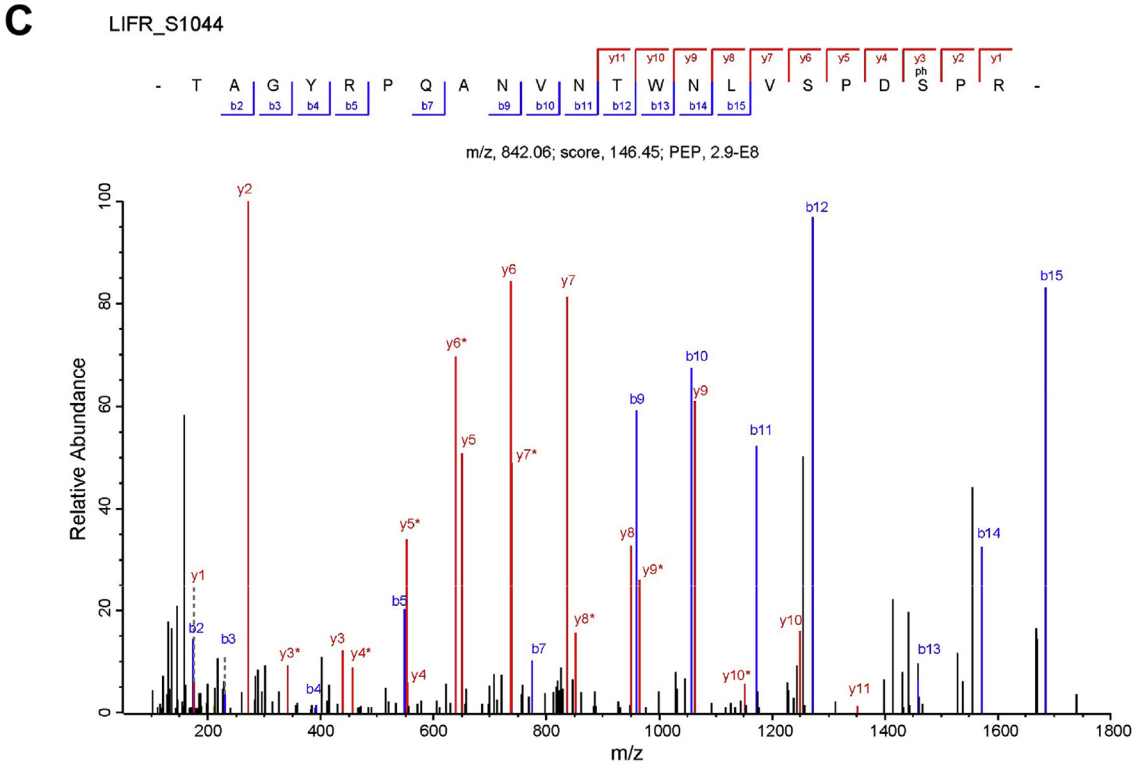

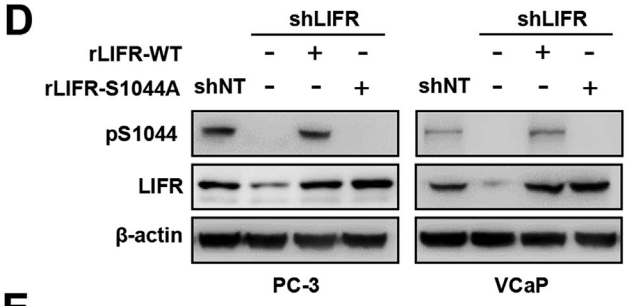

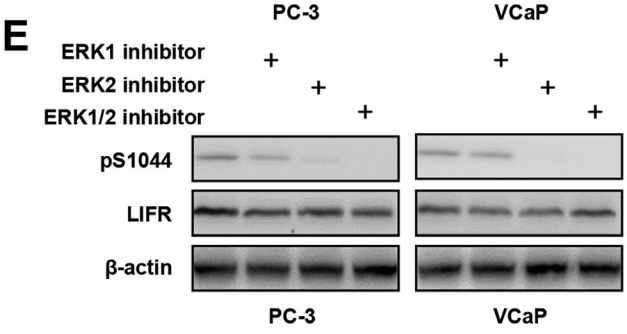

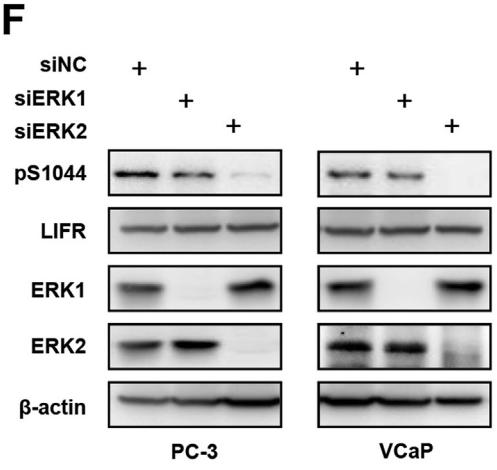

(caption on next page)

and ERK2 is responsible for this PTM [24]. To test how this PTM is regulated in PCa, we used ERK1, ERK2 or ERK1/2 inhibitors to treat PC-3 cells. Consistently, the inhibition of ERK2 alone or of ERK1/2 dramatically reduced the pLIFR-S1044 level (Fig. 3E). In addtion, we used siRNA specifically targeted *ERK1* gene or *ERK2* gene. Consistently, after knockdown of ERK2, pLIFR-S1044 disappeared in PC-3 and VCaP cells (Fig. 3F). These data showed the occurrence of LIFR phosphorylation at S1044 in PC-3 and VCaP cells which depends on ERK2, suggesting that

Fig. 3. Identification of LIFR phosphorylation at S1044 in PCa cells. (A) FLAG-LIFR was immunoprecipitated from PC-3 cells prepared in three independent samples, and LIFR-S1044 was found to be phosphorylated in each sample. **(B)** Western blot analysis of the specificity of the antibody against pS1044-LIFR. Wild-type or S1044A mutant FLAG-LIFR was over-expressed in PC-3 and VCaP cells. **(C)** LC-MS/MS analysis of S1044 phosphorylation. Mass spectrometry analyses of LIFR-associated proteins were performed in PC-3 cells stably expressing FLAG-LIFR. The precursor ion was fragmented by collision-induced dissociation (CID) and analyzed in an ion trap. The database search engine (Andromeda) score was matched to the identified peptide. **(D)** Western blot of wild-type or S1044A mutant LIFR rescued in LIFR knockdown cell lines. Indicated antibodies were used to test endogenous S1044 phosphorylation, LIFR or inner control β-actin. **(E)** The S1044 phosphorylation level and total LIFR were detected by Western blot. ERK1 inhibitor: SC1, 50 nM; ERK2 inhibitor: ulixertinib, 20 nM; ERK1/2 inhibitor: LY3214996, 50 nM. Inhibitor or Mock (0.05% DMSO) was incubated with PC-3 cells or VCaP cells for 6 h and then cells were collected for western blot analysis. Indicated antibodies were used to test endogenous S1044 phosphorylation, LIFR or inner control β-actin. **(F)** Detection of LIFR S1044 phosphorylation after knockdown of ERK1 and ERK2 by siRNA. Indicated antibodies were used to test endogenous S1044 phosphorylation, LIFR or inner control β-actin.

pLIFR-S1044 may play important roles in PCa progression.

3.4. LIFR-S1044 phosphorylation promotes PCa cell proliferation and metastasis in vitro and in vivo

Schiemann et al. previously reported that S1044 phosphorylation by ERK2 marks the activation of LIFR [24], which is recently confirmed in mouse embryonic cells by our team group [23]. Therefore, we hypothesized that LIFR-S1044 phosphorylation could also activate LIFR in PCa cells and contribute to the malignancy of PCa cells, such as by increasing proliferation and metastasis. The CCK-8 data showed that mutant S1044A, which mimicked the depletion of S1044 phosphorylation, reduced cell proliferation to the same level as that of shLIFR cells (Fig. 4A). More importantly, the loss of LIFR-S1044 phosphorylation dramatically affected the metastatic ability of PCa cells (Fig. 4B). Further, a xenograft study was performed by injecting PC-3 shLIFR + rLIFR (wild-type or mutant S1044A) cells into the left groin of nude mice, and the results showed that LIFR-S1044 phosphorylation contributed to PCa cell proliferation and tumor formation *in vivo* (Fig. 4C). Ki67 staining confirmed that the depletion of S1044 phosphorylation reduced cell proliferation *in vivo*, which was consistent with the cell proliferation results *in vitro* (Fig. 4D). We also measured the effect of S1044 phosphorylation on the metastatic ability of PCa cells *in vivo*. Inoculating nude mice with WT and S1044A-mutated cells revealed that the inhibition of LIFR-S1044 phosphorylation greatly diminished metastatic lesion formation in the limbs, indicating that LIFR activation is essential for its function in promoting PCa metastasis (Fig. 4E and F). The metastases were further confirmed by H&E staining (Fig. 4G). Taken together, these results demonstrate that LIFR activation, marked by pLIFR-S1044, is required for PCa cell proliferation and metastasis *in vitro* and *in vivo*.

3.5. LIFR-S1044 phosphorylation promotes AKT signaling and upregulates genes related to cell proliferation, metastasis, invasion and adhesion

There are four major LIFR downstream signaling pathways: PI3K/AKT, hippo/YAP, MAPK and JAK/STAT3 [4,9,10]. In many tumors and immune cells, JAK/STAT3 signaling is overactivated. In spite of the natural deletion of STAT3 in PC-3 cells [25,26], we detected how would LIFR phosphorylation affects the four signaling pathways in PC-3 and VCaP cells. We found that the depletion of LIFR or its phosphorylation at S1044 would heavily block AKT activation while having no effect on YAP or ERK signaling, and slightly decreased STAT3 Y705 phosphorylation (Fig. 5A). Furthermore, we infected PC-3 and VCaP cells with lentivirus to generate stable cell lines overexpressing LIFR, including the wild-type, S1044A mutant or S1044E mutant. Compared with the vehicle group, the overexpression of the wild-type or S1044E promoted AKT activation, while S1044A overexpression resulted in a decreased AKT signal equal to that in the vehicle group. Additionally, we added AKT inhibitor X to the culture medium of S1044E cells and found that the promotion of AKT signaling by the S1044E mutant was abolished or reduced, indicating that S1044E promotes cell proliferation and metastasis by increasing AKT signaling (Fig. 5B). We also tested the effects of the overexpression of LIFR, including the wild type and S1044A S1044E mutants, on PCa cells. We first used the CCK-8 assay to measure cell proliferation capacity. The results showed that the LIFR-S1044A mutant played a dominantnegative role through competition with endogenous LIFR-S1044 phosphorylation, thereby inhibiting the proliferation of PCa cells, while the LIFR-S1044E mutant mimicked constitutive LIFR activation and significantly promoted the proliferation of PCa cells. The proliferation of PCa cells was decreased when AKT inhibitor X blocked AKT activation in S1044E mutants (Fig. 5C & Fig. S3A). Migration, invasion and adhesion assays were applied to test the effects of the S1044A and S1044E mutants on metastatic ability, and the results were as expected; that is, the metastasis of PCa cells was enhanced after LIFR-S1044 phosphorylation, and AKT inhibitor X inhibited the metastasis of S1044E mutants (Fig. 5D & Fig. S3B).

To better understand the downstream targets of LIFR activation, we applied RNA-seq analysis of shLIFR + rS1044A versus shLIFR + rS1044E cells and found that the AKT signaling pathway was one of the most prominent pathways influenced by LIFR- S1044 phosphorylation. Notably, we also found that some metastasis-related pathways, such as those of tight junctions, TGF-β signaling and focal adhesions, were decreased in shLIFR-rS1044A cells (Fig. S3C). Gene Ontology analysis of enriched biological functions showed downregulated genes related to cell migration, focal adhesion and cell motility, indicating that the depletion of LIFR phosphorylation at S1044 would lead to reduced metastatic ability (Fig. 5E). We validated the expression of two genes derived from PI3K-AKT pathway, *CCND1* and *ITGA3*, which corresponded to metastasis and proliferation, respectively (Fig. 5F & Fig. S3D). Taken together, our results confirmed that in PCa, LIFR-S1044 phosphorylation promotes AKT signaling and upregulates the expression of genes related to cell proliferation, metastasis, invasion and adhesion.

3.6. LIFR-S1044 phosphorylation correlates with worse prognosis of metastatic PCa

The investigation of LIFR in tumorigenesis has progressed from exploring cell lines to examine clinical samples. Luo et al. examined 20 types of tumors, including PCa tumors [27]. In contrast to liver cancer, the expression of LIFR was higher in tumor tissue than in adjacent tissue in PCa; however, TCGA data and the results of this study indicate that the levels of LIFR expression in PCa and paired adjacent tissues are not significantly different, suggesting that while LIFR activation plays a more important role in metastatic PCa, while LIFR expression is not a good biomarker for PCa diagnosis.

pLIFR-S1044 and pAKT-S473 were detected in clinical samples, including PCa and adjacent tissues; representative images are shown in Fig. 6A. In detail, the immunostaining signal intensities of pLIFR-S1044 and pAKT-S473 were low in the normal tissues but high in the tumor tissues. We also detected the protein levels and modifications in 6 paired clinical samples by western blot. As shown in Fig. S4, LIFR displayed the similar level between normal and tumor tissues. However, four out of six samples, the pLIFR-S1044 evidently increased in tumor tissues coinciding with pAKT-S473. Furthermore, we calculated the r^2 and p values for the correlations between pLIFR-S1044 and pAKT-S473, and we found a positive correlation between the two markers in 21 clinical samples (Fig. 6B). We recorded the post-operative outcomes between pS1044-high and pS1044-low samples in Table 1.

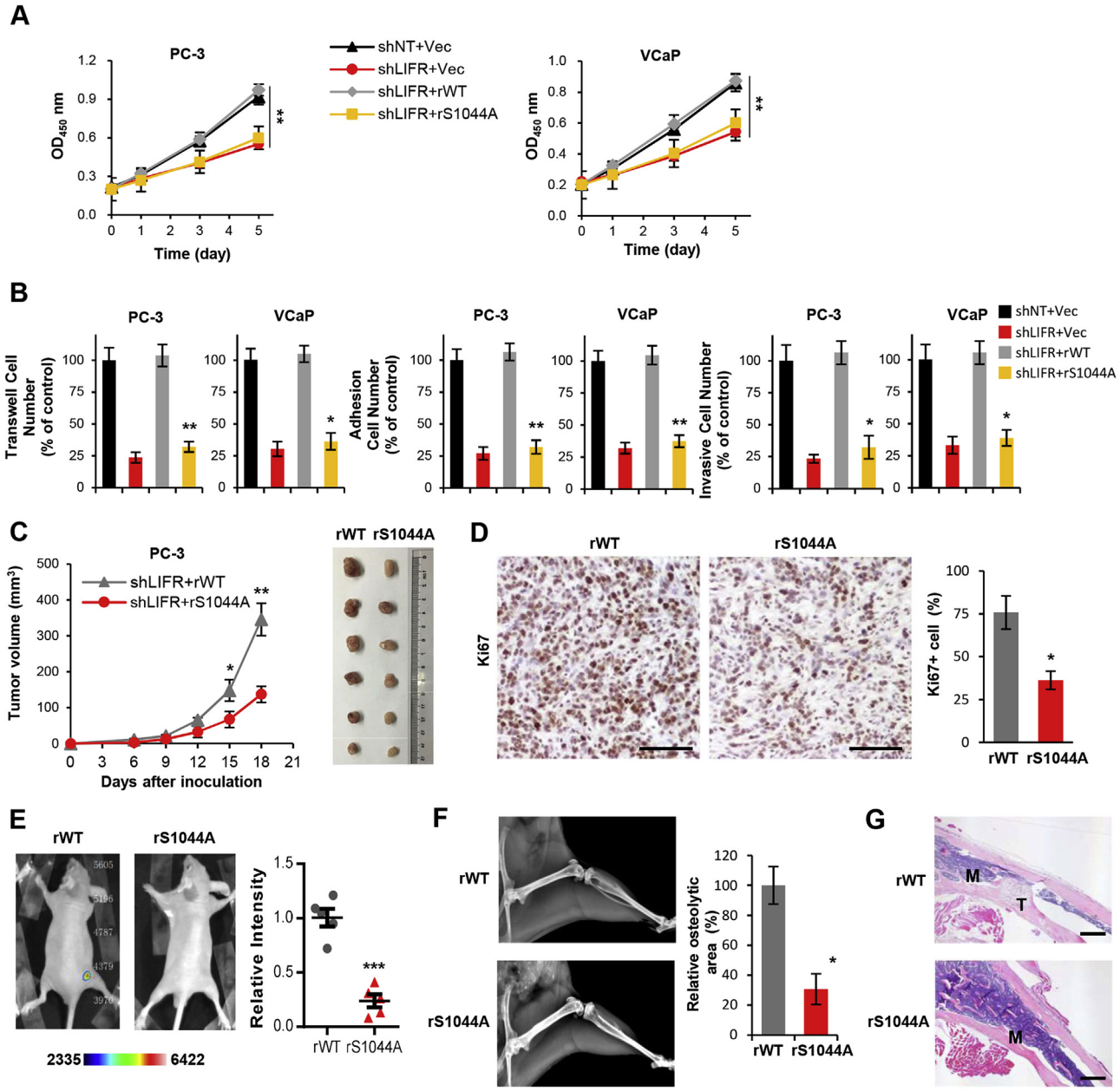

Fig. 4. LIFR-S1044 phosphorylation promotes PCa cell proliferation and metastasis *in vitro* and *in vivo*. **(A)** Measurement of cell growth (left) in LIFR knockdown PC-3 or VCaP cells reintroduced with resistant wild-type or S1044A mutant LIFR. **(B)** The metastasis capacity of LIFR mutant cells was measured by transwell, invasion and adhesion assays. **(C)** PC-3 cells stably expressing mutant LIFR were injected into the left dorsal part of randomized nude mice (n = 6). Tumor growth was examined every 3 days starting on the 6th day (left). The tumors are presented (right). **(D)** Ki67 staining of the xenograft samples was analyzed (left). Positive Ki67 staining in randomly selected sections was calculated and analyzed with corresponding p-values (right). Scale bar: 100 μm. **(E)** Representative BLI images from the rWT or rS1044A mutant groups. Relative BLI quantitation of limb metastasis was shown in the right panel (n = 5 per group). rWT, reconstituted wild type. **(F)** Representative X-ray images for assessing bone metastasis are shown in the left panel, and quantified osteolytic areas are shown in the right panel (n = 5 per group). **(G)** Images of H&E-stained bone sections from the mice, as indicated. T, tumor cell; M, bone marrow. Scale bar: 200 μm. Data are from three independent experiments, presented as the mean ± SEM and were analyzed by unpaired t-tests or two-way ANOVA. *p < 0.05; **p < 0.01; ***p < 0.001.

Consequently, we showed the representative pLIFR-S1044 IHC signal intensities in 8 patients with metastasis. Comparing to primary sites, the distant metastatic sites showed a significant increase of pLIFR-S1044 signal intensities (Fig. 6C). Furthermore, IHC analyses showed that the pLIFR-S1044 levels in tumors from patients (8 cases) with metastatic recurrence were much higher than those in tumors from patients (8 cases) without metastatic recurrence (Fig. 6D). Patients whose tumors had low pLIFR-S1044 levels (157 cases) had significant higher survival duration of 120 months than those whose tumors had high pLIFR-S1044 levels (104 cases) (Fig. 6E).

In light of our results, we propose the following mechanistic model: LIFR-S1044 is phosphorylated by ERK2 which consequently activates the AKT pathway, playing a key role in PCa progression, especially bone metastasis. Downstream genes of the LIFR/AKT axis are upregulated and promote PCa cell proliferation and metastasis (Fig. 6F). Overall, LIFR-S1044 phosphorylation could be applied as a biomarker for predicting metastasis and recurrence in PCa patients. In the future, we will focus on identifying transduction molecules linking LIFR to the AKT signaling pathway and revealing the position of those signaling molecules in the ERK2/LIFR/AKT axis.

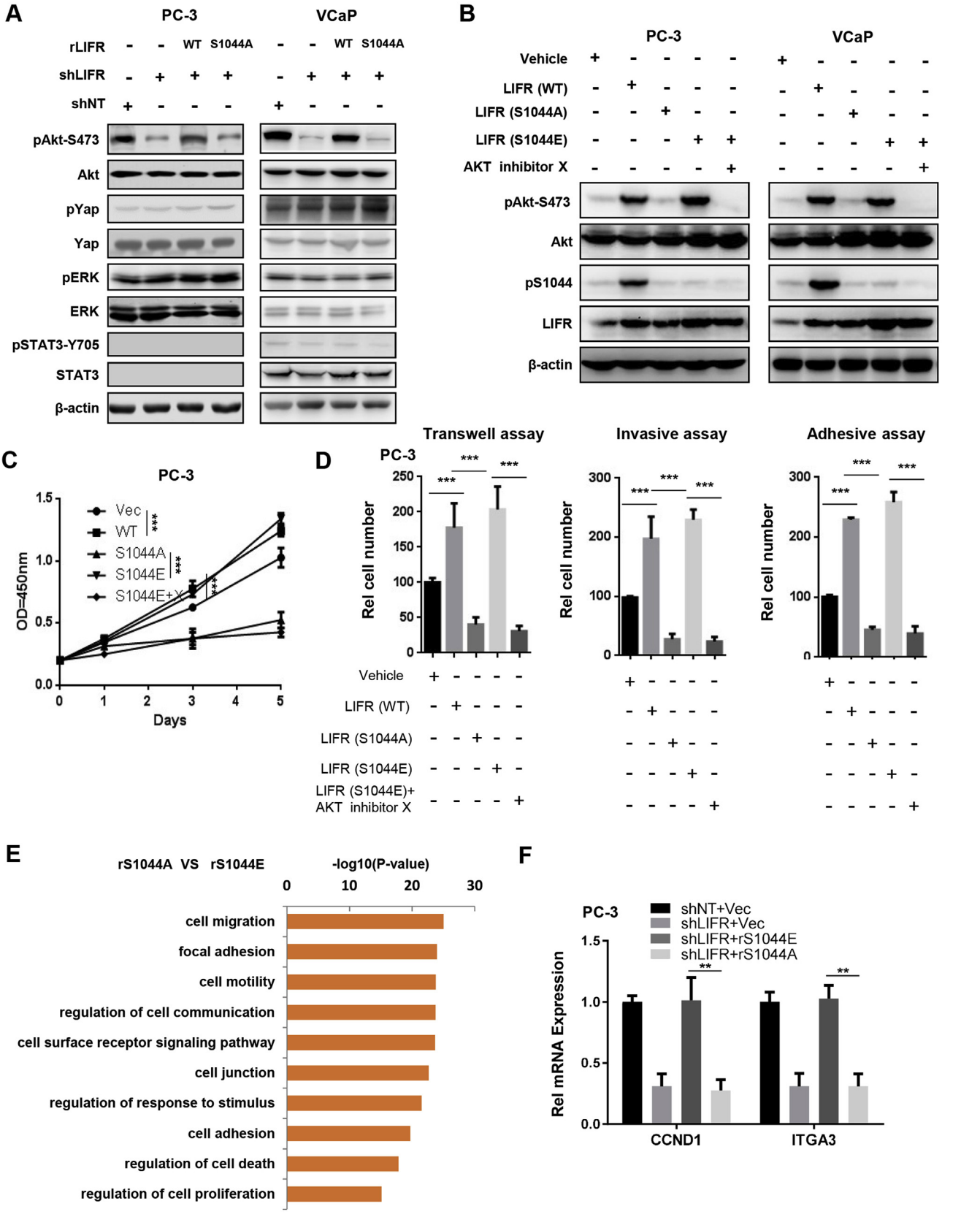

Fig. 5. LIFR-S1044 phosphorylation activates the AKT signaling pathway. (A–B) Western blot was used to examine whether the AKT, Yap, ERK or STAT3 signaling pathways act downstream from LIFR in PCa cells. β-actin was used as an internal control. **(C)** Measurement of the proliferation of wild type, S1044A or S1044E LIFR mutant stable PC-3 cells. **(D)** The metastatic capacity of cells in (C) was measured by transwell, invasion and adhesion assays. **(E)** Detailed pathway enrichment analysis of differentially expressed genes ($p < 0.05$, fold-change > 2.0) in rS1044A mutant cells compared with rS1044E mutant cells. **(F)** Validation of the AKT downstream genes in PC-3 cells. The mRNA expression of β-actin was used as an internal control for normalizing the total mRNA expression levels in different samples. Data are from three independent experiments (C, D, F). Data are presented as the mean ± SD from three independent experiments and were analyzed by unpaired t-tests. ***$p < 0.001$.

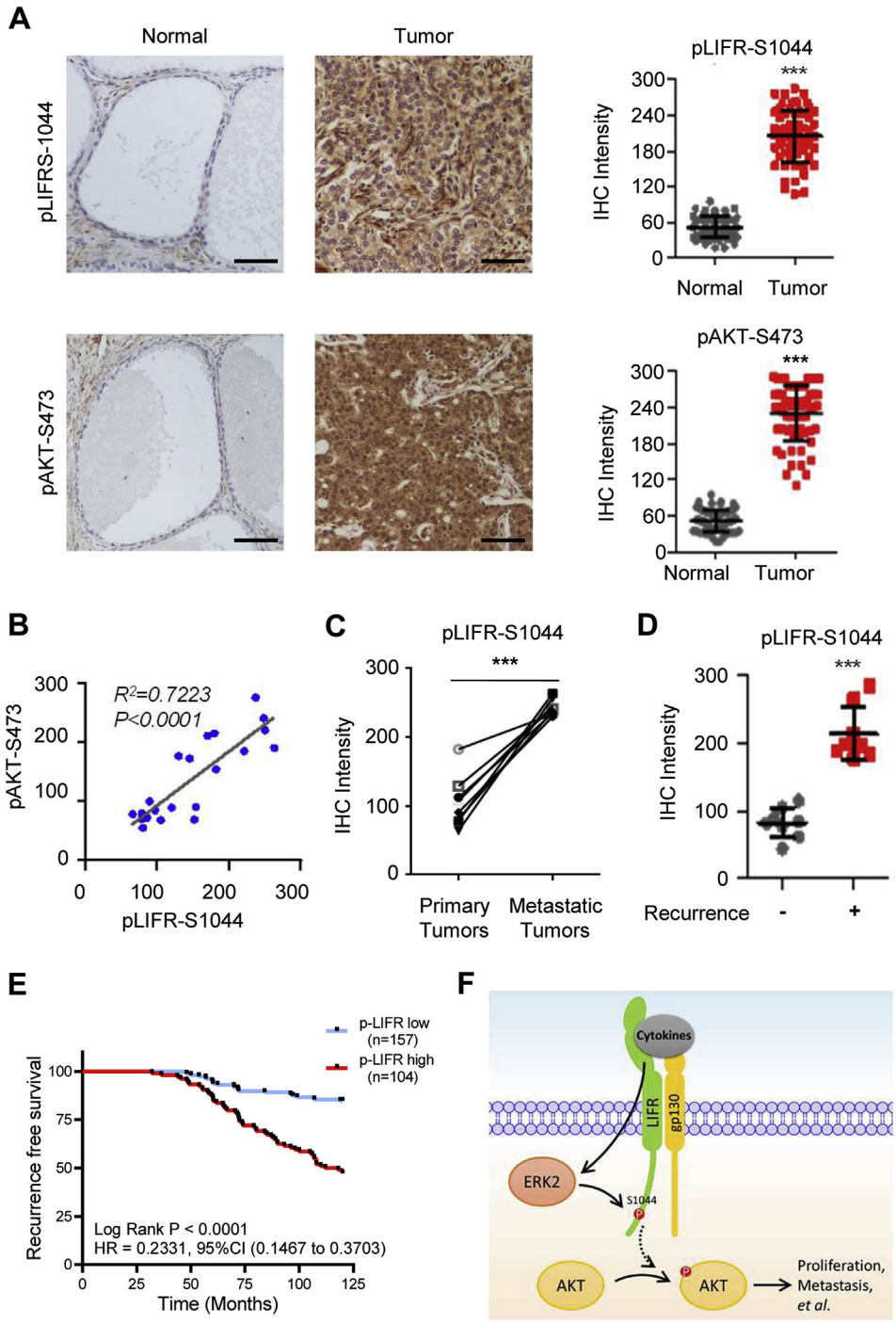

Fig. 6. LIFR phosphorylation at S1044 correlates with prognosis of prostate cancer. (A) IHC staining with antibodies against pLIFR-S1044 and pAKT S473 was performed in tumor tissues and paired adjacent normal tissues. Left, representative images of prostate cancer sample. Scale bar: 100 μm. Right, semiquantitative scoring was performed, and the signal intensities of pLIFR-S1044 and pAKT S473 levels were quantified using the Motic Images Advanced software, followed by statistical analysis. A total of 65 tumor tissues and 65 adjacent normal tissues were analyzed. The mean value of multiple samples and standard deviation are presented. **(B)** A positive correlation of pLIFR-S1044 with pAKT S473 was found, with $r^2 = 0.7223$ and $p < 0.0001$. **(C)** IHC staining was performed in primary tumors and paired metastatic tumors from 16 PCa patients with distant metastasis using an anti-pLIFR-S1044 antibody. The staining scores of the primary PCa specimens were compared with those of the metastatic PCa specimens. **(D)** IHC staining was performed in tumors from PCa patients with or without metastatic recurrence using anti-pLIFR-S1044 antibody. The staining scores of pLIFR-S1044 were compared between the patients with metastatic recurrence (n = 20) and the patients without metastatic recurrence (n = 20). **(E)** The survival durations of 261 PCa patients with low (staining scores 0–150, blue curve) versus high (staining scores 151–300, red curve) pLIFR-S1044 levels (low, 157 patients; high, 104 patients) were compared. Landmark represents censored (alive at last clinical follow-up) patients. **(F)** The mechanism by which the ERK2/LIFR/AKT axis modulates PCa progression. Data are presented as the mean ± SEM (A, D) and were analyzed by unpaired t-tests (A, C, D), the Pearson product moment correlation test (B) or the log-rank test (E). *p < 0.05; **p < 0.01; ***p < 0.001. (For interpretation of the references to color in this figure legend, the reader is referred to the Web version of this article.)

4. Discussion

LIFR is a type I cytokine receptor, and most type I cytokine receptors, such as OSMR, GCSFR, IL6R and LIFR, form a heterodimer complex with gp130 to deliver extracellular signals. LIFR has been suggested to play multiple roles in different types of cancers. The roles of LIFR signaling in PCa are still largely unknown. A recent report has shown that histone methyltransferase KMT2D sustains prostate carcinogenesis and metastasis via epigenetically activating LIFR and KLF4 [18]. In this study, we identified LIFR as a tumor promoter that is required for PCa proliferation and metastasis. The depletion of LIFR in PC-3 and VCaP cells significantly attenuated cell proliferation and metastatic abilities. Moreover, xenograft and bone metastasis models showed the functions of LIFR in tumor growth and metastasis in mouse experiment. Clinically, both TCGA database and PCa patients' samples from our hospital presented no correlation between LIFR expression and patients' survival duration, indicating LIFR activation, but not expression, was significantly correlated with PCa progression and recurrence.

As a cell membrane located receptor, the extracellular domain of LIFR binds ligands, and in turn, the intracellular domain will produce a variety of translational modifications, such as phosphorylation and acetylation, which usually facilitate dimer formation or recruit kinases to promote downstream transcription factor activation. Multiple serine phosphorylation sites in the C-terminus of LIFR, including S927, S1041, S1044, S1059 and S1077 have been identified [24]. Here, we evaluated

LIFR serine phosphorylation at its C-terminus and identified frequent S1044 phosphorylation occurring, which has been reported as a marker of LIFR activation. To clarify the function of S1044 phosphorylation in PCa, we produced dominant-positive (E) and dominant-negative (A) S1044 mutants and verified their functions both *in vitro* and *in vivo*. Besides, we applied a specific antibody against S1044 phosphorylation to clinical samples and found that a higher S1044 phosphorylation level correlated with metastasis and malignancy in PCa. These results suggest that PCa progression can be identified using a specific antibody against S1044 phosphorylation.

Consequently, how would LIFR phosphorylation affects downstream signaling to promote PCa proliferation and metastasis? In breast cancer, the YAP signaling pathway, rather than the JAK/STAT3 signaling pathway, is downstream from LIFR, which is consistent with the view that LIFR mediates the heterogeneity of tumors [28]. However, a recent report showed that histone deacetylase (HDAC) inhibitors transcriptionally activated LIFR could limit response to HDAC inhibition through LIFR-JAK1-STAT3 signaling in breast cancer [29]. Luo et al. further confirmed the downregulation of LIFR expression in liver cancer and found that LIFR functions through downregulating the AKT signaling pathway via an unknown mechanism [12]. PCa progression involves multiple signaling pathways, such as mTOR, TGF-β, PI3K/AKT, and Wnt/β-catenin signaling pathways. However, how LIFR activation regulates PCa progression through which downstream signaling remains elusive.

To date, several downstream signaling pathways of LIFR have been identified, including JAK/STAT3, PI3K/AKT, hippo/YAP and MAPK. We analyzed the levels of pAKT, pYAP, pERK and pSTAT3 to further confirm the pathways regulated by LIFR in PCa cells. By reintroducing S1044 mutants (including S1044A and S1044D) into LIFR-depleted PCa cells and generating cell lines with stably rescued LIFR expression, LIFR-S1044 phosphorylation-mediated biological consequences and corresponding signaling pathways were determined. The results excluded the involvement of other cascades except the AKT pathway. The functional and diagnostic links between PCa malignance and AKT activation have been established for over a decade [30–34]. The AKT signaling pathway plays a critical role in controlling cell proliferation and metastasis [30,32,33]. The maintenance of prostate cancer stem-like cells requires AKT pathway as well [35]. Our results identified a crucial upstream activator responsible for stimulating AKT signaling pathway in prostate cancer.

Receptor mediated signal transduction is abundantly marked by the PTMs on the receptors especially phosphorylation [36]. Our work highlights the potential of LIFR-S1044 phosphorylation as an efficient biomarker for monitoring PCa progression. Remarkably, pLIFR-S1044 can be detected not only by biopsy but also in blood samples, as LIFR has a soluble form in serum [37,38].

Conflicts of interest

The authors declare that they have no competing interests.

Acknowledgments

This study was supported by funds from the Hundred Talent Program of Guangzhou University (to Dr. Xiongjun Wang & Dr. Yunbo Qiao), National Natural Science Foundation of China (No.81570607, No. 81170697,to Dr. Xiang Wang), and Shanghai Shenkang Hospital Development Center Fund (No. 16CR2003A,to Dr. Xiang Wang).

Appendix A. Supplementary data

Supplementary data to this article can be found online at https://doi.org/10.1016/j.canlet.2019.02.042.

References

[1] R.L. Siegel, K.D. Miller, A. Jemal, Cancer statistics, 2017, CA A Cancer J. Clin. 67 (2017) 7–30.
[2] J.R. Walczak, M.A. Carducci, Prostate cancer: a practical approach to current management of recurrent disease, Mayo Clin. Proc. 82 (2007) 243–249.
[3] M.N. Thobe, R.J. Clark, R.O. Bainer, S.M. Prasad, C.W. Rinker-Schaeffer, From prostate to bone: key players in prostate cancer bone metastasis, Cancers 3 (2011) 478–493.
[4] T. Kishimoto, S. Akira, M. Narazaki, T. Taga, Interleukin-6 family of cytokines and gp130, Blood 86 (1995) 1243–1254.
[5] T. Taga, T. Kishimoto, gp130 and the interleukin-6 family of cytokines, Annu. Rev. Immunol. 15 (1997) 797–819.
[6] J.G. Zhang, Y. Zhang, C.M. Owczarek, L.D. Ward, R.L. Moritz, R.J. Simpson, K. Yasukawa, N.A. Nicola, Identification and characterization of two distinct truncated forms of gp130 and a soluble form of leukemia inhibitory factor receptor alpha-chain in normal human urine and plasma, J. Biol. Chem. 273 (1998) 10798–10805.
[7] C.J. Auernhammer, S. Melmed, Leukemia-inhibitory factor-neuroimmune modulator of endocrine function, Endocr. Rev. 21 (2000) 313–345.
[8] N.A. Sims, R.W. Johnson, Leukemia inhibitory factor: a paracrine mediator of bone metabolism, Growth Factors 30 (2012) 76–87.
[9] A. Hergovich, YAP-Hippo signalling downstream of leukemia inhibitory factor receptor: implications for breast cancer, Breast Cancer Res. 14 (2012) 326.
[10] D.H. Chen, Y.T. Sun, Y.K. Wei, P.J. Zhang, A.H. Rezaeian, J. Teruya-Feldstein, S. Gupta, H. Liang, H.K. Lin, M.C. Hung, L. Ma, LIFR is a breast cancer metastasis suppressor upstream of the Hippo-YAP pathway and a prognostic marker, Nat. Med. 18 (2012) 1511–1517.
[11] R.W. Johnson, E.C. Fingers, M.M. Olcina, M. Vilalta, T. Aguilera, Y. Miao, A.R. Merkel, J.R. Johnson, J.A. Sterling, J.Y. Wu, A.J. Giaccia, Induction of LIFR confers a dormancy phenotype in breast cancer cells disseminated to the, bone marrow, Nat. Cell Biol. 18 (2016) 1078–1089.
[12] Q. Luo, C. Wang, G.Z. Jin, D.S. Gu, N. Wang, J. Song, H.J. Jin, F.Y. Hu, Y.R. Zhang, T.X. Ge, X.S. Huo, W. Chu, H.Q. Shu, J.Y. Fang, M. Yao, J.R. Gu, W.M. Cong, W.X. Qin, LIFR functions as a metastasis suppressor in hepatocellular carcinoma by negatively regulating phosphoinositide 3-kinase/AKT pathway, Carcinogenesis 36 (2015) 1201–1212.
[13] Y. Okamura, S. Nomoto, M. Kanda, Q.Y. Li, Y. Nishikawa, H. Sugimoto, N. Kanazumi, S. Takeda, A. Nakao, Leukemia inhibitory factor receptor (LIFR) is detected as a novel suppressor gene of hepatocellular carcinoma using double-combination array, Cancer Lett. 289 (2010) 170–177.
[14] F.F. Zhang, K.T. Li, M.X. Pan, W.D. Li, J. Wu, M.Y. Li, L. Zhao, H. Wang, miR-589 promotes gastric cancer aggressiveness by a LIFR-PI3K/AKT-c-Jun regulatory feedback loop, J. Exp. Clin. Cancer Res. 37 (2018) 152.
[15] F. Blanchard, E. Tracy, J. Smith, S. Chattopadhyay, Y.P. Wang, W.A. Held, H. Baumann, DNA methylation controls the responsiveness of hepatoma cells to leukemia inhibitory factor, Hepatology 38 (2003) 1516–1528.
[16] H.X. Wu, X. Cheng, X.Q. Jing, X.P. Ji, X.Z. Chen, Y.Q. Zhang, Y.G. He, K. Liu, F. Ye, H.X. Sun, H.J. Gao, Z.J. Song, H. Wu, X.J. Zhang, T. Zhang, R. Zhao, LIFR promotes tumor angiogenesis by up-regulating IL-8 levels in colorectal cancer, Biochim. Biophys. Acta (BBA) - Mol. Basis Dis. 1864 (2018) 2769–2784.
[17] H.W. Guo, Y.B. Cheng, M. Martinka, K. McElwee, High LIFr expression stimulates melanoma cell migration and is associated with unfavorable prognosis in melanoma, Oncotarget 6 (2015) 25484–25498.
[18] S. Lv, L. Ji, B. Chen, S. Liu, C. Lei, X. Liu, X. Qi, Y. Wang, E. Lai-Han Leung, H. Wang, L. Zhang, X. Yu, Z. Liu, Q. Wei, L. Lu, Histone methyltransferase KMT2D sustains prostate carcinogenesis and metastasis via epigenetically activating LIFR and KLF4, Oncogene 37 (2018) 1354–1368.
[19] D.S. Chandrashekar, B. Bashel, S.A.H. Balasubramanya, C.J. Creighton, I. Ponce-Rodriguez, B. Chakravarthi, S. Varambally, UALCAN: a portal for facilitating tumor subgroup gene expression and survival analyses, Neoplasia 19 (2017) 649–658.
[20] G.C. Elson, E. Lelievre, C. Guillet, S. Chevalier, H. Plun-Favreau, J. Froger, I. Suard, A.B. de Coignac, Y. Delneste, J.Y. Bonnefoy, J.F. Gauchat, H. Gascan, CLF associates with CLC to form a functional heteromeric ligand for the CNTF receptor complex, Nat. Neurosci. 3 (2000) 867–872.
[21] P.C. Heinrich, I. Behrmann, S. Haan, H.M. Hermanns, G. Muller-Newen, F. Schaper, Principles of interleukin (IL)-6-type cytokine signalling and its regulation, Biochem. J. 374 (2003) 1–20.
[22] M. Mann, O.N. Jensen, Proteomic analysis of post-translational modifications, Nat. Biotechnol. 21 (2003) 255–261.
[23] X.J. Wang, Y. Qiao, M.M. Xiao, L. Wang, J. Chen, W. Lv, L. Xu, Y. Li, Y. Wang, M.D. Tan, C. Huang, J. Li, T.C. Zhao, Z. Hou, N. Jing, Y.E. Chin, Opposing roles of acetylation and phosphorylation in LIFR-dependent self-renewal growth signaling in mouse embryonic stem cells, Cell Rep. 18 (2017) 933–946.
[24] W.P. Schiemann, L.M. Graves, H. Baumann, K.K. Morella, D.P. Gearing, M.D. Nielsen, E.G. Krebs, N.M. Nathanson, Phosphorylation of the human leukemia inhibitory factor (LIF) receptor by mitogen-activated protein kinase and the regulation of LIF receptor function by heterologous receptor activation, P. Natl. Acad. Sci. USA 92 (1995) 5361–5365.
[25] M.T. Spiotto, T.D.K. Chung, STAT3 mediates IL-6-induced growth inhibition in the human prostate cancer cell line LNCaP, Prostate 42 (2000) 88–98.
[26] S. Mori, K. Murakami-Mori, A. Bonavida, Oncostatin M (OM) promotes the growth of DU 145 human prostate cancer cells, but not PC-3 or LNCaP, through the signaling of the OM specific receptor, Anticancer Res. 19 (1999) 1011–1015.
[27] Q. Luo, Y.R. Zhang, N. Wang, G.Z. Jin, H.J. Jin, D.S. Gu, X.M. Tao, X.S. Huo,

T.X. Ge, W.M. Cong, C. Wang, W.X. Qin, Leukemia inhibitory factor receptor is a novel immunomarker in distinction of well-differentiated HCC from dysplastic nodules, Oncotarget 6 (2015) 6989–6999.
[28] E. Iorns, T.M. Ward, S. Dean, A. Jegg, D. Thomas, N. Murugaesu, D. Sims, C. Mitsopoulos, K. Fenwick, I. Kozarewa, C. Naceur-Lombarelli, M. Zvelebil, C.M. Isacke, C.J. Lord, A. Ashworth, H.J. Hnatyszyn, M. Pegram, M. Lippman, Whole genome in vivo RNAi screening identifies the leukemia inhibitory factor receptor as a novel breast tumor suppressor, Breast Canc. Res. Treat. 135 (2012) 79–91.
[29] H.L. Zeng, J. Qu, N. Jin, J. Xu, C.C. Lin, Y. Chen, X.Y. Yang, X. He, S. Tang, X.J. Lan, X.T. Yang, Z.Q. Chen, M. Huang, J. Ding, M.Y. Geng, Feedback activation of leukemia inhibitory factor receptor limits response to histone deacetylase inhibitors in breast cancer, Cancer Cell 30 (2016) 459–473.
[30] S.N. Malik, M. Brattain, P.M. Ghosh, D.A. Troyer, T. Prihoda, R. Bedolla, J.I. Kreisberg, Immunohistochemical demonstration of phospho-Akt in high Gleason grade prostate cancer, Clin. Cancer Res. 8 (2002) 1168–1171.
[31] S. Shukla, G.T. Maclennan, D.J. Hartman, P. Fu, M.I. Resnick, S. Gupta, Activation of PI3K-Akt signaling pathway promotes prostate cancer cell invasion, Int. J. Cancer 121 (2007) 1424–1432.
[32] J.I. Kreisberg, S.N. Malik, T.J. Prihoda, R.G. Bedolla, D.A. Troyer, S. Kreisberg, P.M. Ghosh, Phosphorylation of Akt (Ser(473)) is an excellent predictor of poor clinical outcome in prostate cancer, Cancer Res. 64 (2004) 5232–5236.
[33] J.R. Graff, B.W. Konicek, A.M. McNulty, Z.J. Wang, K. Houck, S. Allen, J.D. Paul, A. Hbaiu, R.G. Goode, G.E. Sandusky, R.L. Vessella, B.L. Neubauer, Increased AKT activity contributes to prostate cancer progression by dramatically accelerating prostate tumor growth and diminishing p27(Kip1) expression, J. Biol. Chem. 275 (2000) 24500–24505.
[34] P.K. Majumder, W.R. Sellers, Akt-regulated pathways in prostate cancer, Oncogene 24 (2005) 7465–7474.
[35] A. Dubrovska, S. Kim, R.J. Salamone, J.R. Walker, S.M. Maira, C. Garcia-Echeverria, P.G. Schultz, V.A. Reddy, The role of PTEN/Akt/PI3K signaling in the maintenance and viability of prostate cancer stem-like cell populations, P. Natl. Acad. Sci. USA 106 (2009) 268–273.
[36] L.P. Kane, J. Lin, A. Weiss, Signal transduction by the TCR for antigen, Curr. Opin. Immunol. 12 (2000) 242–249.
[37] S. Rosejohn, P.C. Heinrich, Soluble receptors for cytokines and growth-factors - generation and biological function, Biochem. J. 300 (1994) 281–290.
[38] M.J. Layton, B.A. Cross, D. Metcalf, L.D. Ward, R.J. Simpson, N.A. Nicola, A major binding-protein for leukemia inhibitory factor in normal mouse serum - identification as a soluble form of the cellular receptor, P. Natl. Acad. Sci. USA 89 (1992) 8616–8620.